

MIGRATING NEPTUNE-CLASS BODIES AS A SOURCE OF LARGE TERRESTRIAL PLANETS

H. Lammer⁽¹⁾, F. Selsis⁽²⁾, I. Ribas^(3,4), H. I. M. Lichtenegger⁽¹⁾, T. Penz^(1,5), E. F. Guinan⁽⁴⁾,
S. J. Bauer⁽⁵⁾, W. W. Weiss⁽⁶⁾

⁽¹⁾*Space Research Institute, Austrian Academy of Sciences, Schmiedlstr. 6, 8042 Graz, Austria*
Email: helmut.lammer@oeaw.ac.at, herbert.lichtenegger@oeaw.ac.at

⁽²⁾*Centro de Astrobiología (INTA-CSIC), Carretera de Ajalvir, km 4, 28850, Torrejón de Ardoz, Madrid, Spain*
Email: selsisf@inta.es

⁽³⁾*Departament d'Astronomia i Meteorologia, Universitat de Barcelona, Av. Diagonal 647, 08028 Barcelona, Spain*
Email: iribas@am.ub.es

⁽⁴⁾*Department of Astronomy and Astrophysics, Villanova University, Villanova, PA 19085, USA*
Email: edward.guinan@ucis.vill.edu

⁽⁵⁾*Institute for Geophysics, Astrophysics and Meteorology, University of Graz, Universitätsplatz 5, 8010 Graz, Austria,*
Email: siegfried.bauer@kfunigraz.ac.at, thomas.penz@kfunigraz.ac.at

⁽⁶⁾*Department for Astronomy, University of Vienna, Türkenschanzstr. 17, A-1180 Vienna, Austria*
Email: weiss@astro.univie.ac.at

ABSTRACT

After the discovery of more than 100 exosolar Jupiter-class planets the detection of Neptune-size and large terrestrial-like bodies will be the next major step in the search for exoplanets. Space-borne telescopes like COROT and Eddington using high precision photometry and the transit technique, will have the capability to detect exoplanets with sizes of 1.5-4 Earth radii at distances between 0.3-1 au. Current theoretical models indicate that the discovered large exoplanets orbiting close to their central star may have either migrated inward from greater distances, or may have formed at their present orbit. In recent studies of close-in giant exoplanets the radiative effective temperature, which is not physically relevant for atmospheric loss processes was used to estimate atmospheric evaporation rates [1, 2]. Therefore, these studies lead to significant underestimations of thermal atmospheric escape rates with values $\leq 10^3 \text{ g s}^{-1}$ and to conclusions of long-term atmospheric stability [2]. However, the exosphere temperature, which controls the thermal escape in an upper atmosphere, is usually much higher than the effective temperature, since upper planetary atmospheres are mainly controlled by absorption of X-rays and extreme ultraviolet (XUV) radiation [3]. In this study, a scaling relation from solar system planets is used to estimate the exospheric temperature for exoplanets. This relation is based on the assumption of equilibrium between the XUV heat input and downward heat transport by conduction. We found that large exospheric temperatures, which are typical for hydrogen-dominated thermospheres, develop at close orbital distances to their host stars. These exosphere temperatures lead to hydrodynamic energy limited escape. Further, we estimate the protection effect of upper atmospheres due to an assumed intrinsic planetary magnetic field and simulate atmospheric ion pick up fluxes by a test particle model, which was

successfully applied on Venus and Mars [4]. We found that “Hot Neptune’s” may lose their entire hydrogen atmospheres by thermal and non-thermal atmospheric escape processes and can evolve into a new type of terrestrial planet, after the development of secondary atmospheres by out-gassing their remaining ice-rocky cores. Moreover, our mass loss estimations applied to Jupiter-class exoplanets agree well with the recent H Lyman α detection of an extended exosphere at HD 209458b and its observation based estimated loss rate of about 10^{10} g s^{-1} [5].

1. XUV HEATING OF THERMOSPHERES

In previous studies of close-in giant exoplanets the radiative effective temperature

$$T_{\text{eff}} = \left[\frac{S(1-A)}{4\sigma D^2} \right]^{\frac{1}{4}}, \quad (1)$$

which depends on the stellar luminosity S , the planetary albedo A , the Stefan-Boltzmann constant σ and orbital distance D (in astronomical units) was used to estimate atmospheric loss rates [1, 2]. However, the exosphere temperature T_{∞} which controls the thermal escape, is usually much higher than T_{eff} . Table 1 shows the planetary effective temperature T_{eff} of various planets in our solar system compared to their dayside surface temperature T_s , mesopause temperature T_0 (at the base of the thermosphere) and exosphere temperature T_{∞} . As an example, Jupiter’s $T_{\infty} \approx 1000 \text{ K}$ is close to T_{eff} of 51 Peg b of about 1300 K. Even Earth’s T_{∞} can reach T_{eff} of 51 Peg b during high solar activity. The question is then, what is T_{∞} of 51 Peg b and other close-in giant exoplanets? Observations by various spacecraft indicate that T_{∞} depends on terrestrial planets solely on the XUV flux into planetary thermospheres but additional thermospheric heating sources caused by accelerated particles and

atmospheric gravity waves become important for giant planets in the outer Solar System.

Table 1. T_{eff} , T_s , T_0 and T_∞ on various planets.

Planet	T_{eff} [K]	T_s [K]	T_0 [K]	T_∞ [K]
Venus	232	750	160	300
Earth	255	288	180	1000-1500
Mars	217	225	120	220
Jupiter	124	-	125	700-1000
Saturn	95	-	95	800-900
Uranus	59	-	52	750
Neptune	59	-	52	750

Since, these additional heating sources are not well understood even at the giant planets in our Solar System we estimate only the exospheric XUV heating contribution ($T_{XUV\infty}$) based on an approximate solution of the heat balance equation in planetary upper atmospheres. Below the exobase (in the thermosphere), the heat absorbed per unit volume from XUV radiation Q_{XUV} is balanced by the divergence of a conductive heat flux F [3]. We neglect cooling by infra-red (IR) radiating molecules because such constituents are not numerous at thermospheric altitudes. In the case of hydrogen rich atmospheres, we neglect also IR-cooling by H_3^+ molecular ions, although this species is observed over the small auroral areas of the giant planets. Because, H_2^+ ions are produced mainly at the polar caps by energetic electrons, where they react with H_2 to form H_3^+ , for close-in exoplanets H_2 is dissociated by the stronger radiation before the molecule gets ionized, so that H_3^+ ions may not be produced in large amounts. By these assumptions one gets $\nabla F = Q_{XUV}$, where $F = -K(T) dT/dz$, with $K(T)$ the thermal conductivity and dT/dz the temperature gradient with altitude and $Q_{XUV} = n \sigma_a \varepsilon I_{XUV\infty} e^{-\tau}$ with n the number density of the absorbing constituent, σ_a its average absorption cross section, ε the heating efficiency of solar XUV radiation of intensity $I_{XUV\infty}$ outside the atmosphere and $\tau = f(n, \sigma_a, z)$ the optical depth. The integrated form of these relations is

$$\int_{z_0}^{z_\infty} e I_{XUV\infty} (1 - e^{-\tau}) dz = \int_{T_0}^{T_{XUV\infty}} K(T) dT, \quad (2)$$

where z_0 is the mesopause altitude at the base of the thermosphere and z_∞ is the exobase altitude. Experimental data and quantum mechanical calculations show that for atmospheric gases the thermal conductivity coefficient $K(T) = K_0 T^s$, where s depends on the thermospheric composition [3].

Integration of Eq. 2 leads to

$$\frac{e I_{XUV\infty}}{n(z_\infty) \mathbf{s}_a} \approx K_0 (T_{XUV\infty}^{s+1} + T_0^{s+1}). \quad (3)$$

If one assumes that $\tau \rightarrow 0$ at z_∞ in the exosphere and $\tau \rightarrow \infty$ at z_0 at the base of the thermosphere and $[n(z_\infty) \sigma_a]^{-1} \gg z_\infty - z_0$ because the densities in the exosphere are in the order of less than 10^8 cm^{-3} and σ_a is about 10^{17} cm^2 . One can substitute for $n(z_\infty)$ at the exobase $n \approx (\sigma_c H)^{-1}$ which derives from the exospheric condition that the mean free path is of the order of the locale scale height $H = kT_\infty/mg$, where k is the Boltzmann constant, m is the mean mass and g the gravitational acceleration at the exobase and σ_c is the collision cross section. Thus, we find the exosphere temperature from Eq. 3 as

$$T_{XUV\infty}^s \approx \frac{e I_{EUV} k \mathbf{s}_c}{K_0 m g \mathbf{s}_a} + T_0^s. \quad (4)$$

If planets 1 and 2 have thermospheres with comparable gas compositions, the following scaling relation can be used [6]

$$\frac{(T_{XUV\infty}^s - T_0^s)_1}{(T_{XUV\infty}^s - T_0^s)_2} \approx \frac{I_{XUV1} g_2}{I_{XUV2} g_1}. \quad (5)$$

Eq. 5 shows that $T_{XUV\infty}$ depends on I_{XUV} , which decreases with distance from the star, and on g , which is related to the mass of the planet. Before we estimate $T_{XUV\infty}$ for exoplanets we discuss thermal escape processes, which can occur by our obtained $T_{XUV\infty}$ values.

2. JEANS ESCAPE

Jeans proposed a model of an isothermal atmosphere in diffusive equilibrium which gives accurate thermal atmospheric escape rates and is valid as long as the thermal escape parameter $X = (u_\infty/u_0)^2$ at the exobase does not reach values of about 1.5 [6]. u_∞ is the escape velocity of the planet and $u_0 = (2kT_\infty/m)^{1/2}$ is the most probable velocity of exospheric particles. The Jeans equation for the escape flux is

$$F_{\text{Jeans}} = \left(\frac{u_0}{2p^{1/2}} \right) n_\infty (1 + X_\infty) e^{-X_\infty}, \quad (6)$$

where n_∞ is the density and X_∞ is the escape parameter of the escaping constituent at the exobase. If X reaches 1.5 the exosphere becomes unstable and diffusive equilibrium no longer applies [7, 8]. For $X \geq 1.5$, the escape flux at the exobase level is given by the Jeans equation. For $X \leq 1.5$ the thermal energy exceeds the gravitational potential energy ($3kT_\infty > 2MmG/r$, where

G is the gravitational constant and M is the planetary mass) leading to the onset of pure hydrogen winds only limited by the incoming XUV flux [8]. Therefore, the scaling law in Eq. 5 for $T_{XUV\infty}$ is not applied for $X \leq 1.5$ because mass loss can no longer be estimated from the Jeans equation and hydrodynamic escape must be considered.

3. HYDRODYNAMIC ESCAPE

As discussed before, if the escape parameter X reaches values at the exobase of about 1.5 corresponding to exospheric temperatures for giant exoplanets above 10000 K, the internal energy of the atmospheric gas is greater than the depth of the gravitational potential in which it is situated. The gas should therefore flow off the planet in bulk rather than merely evaporate from the exobase so that the escape is a process similar in many respects to the supersonic flow of plasma from the solar wind [8]. By considering a dynamically expanding non-viscous gas of constant molecular weight, in which the pressure is isotropic, the steady state equations and energy conservation can be written as

$$\nabla \cdot (nu) = 0, \quad (7)$$

$$mn(u \cdot \nabla)u + \nabla(nkT) = nmg, \quad (8)$$

$$\nabla \cdot (K\nabla T) = \nabla \cdot \left[\frac{5}{2}nkTu + n \left(\frac{mu^2}{2} \right) u \right] - nmg \cdot u - Q_{XUV}, \quad (9)$$

where u is the bulk velocity of the gas, g the acceleration of gravity, K the thermal conductivity parameter and Q_{XUV} is the volume-heating rate caused by the XUV radiation. To apply these equations to a dense thermosphere one can make the following assumptions [8]: (1) At a distance r_0 in the upper atmosphere, the temperature is fixed at T_0 and (2) the atmosphere is sufficiently dense that the optical depth of the lower boundary to XUV is much greater than 1. One can assume that the XUV flux is absorbed in a distance at a higher altitude r_1 . Since, there is little energy deposited above r_1 and the gas is continually expanding, the temperature T_1 declines as $r \rightarrow \infty$. The pressure of the gas also declines toward zero because, the gas must expand according to a critical solution of the hydrodynamic equations. For the estimation of the expansion radius r_1 and the corresponding escape rates we define the following dimensionless parameters (8) for the flux ζ

$$\mathbf{z} = L_{Hydro} \left(\frac{k^2 T_0}{\mathbf{k}_0 GMm} \right), \quad (10)$$

and for the energy β

$$\mathbf{b} = I_{XUV} \left(\frac{GMm}{kT_0^2 \mathbf{k}_0} \right), \quad (11)$$

where I_{Hydro} is the hydrodynamic energy limited loss rate and I_{XUV} is the energy rate in $\text{erg cm}^{-2} \text{s}^{-1}$ supplied by the XUV. I_{XUV} had been suitably averaged over the planetary sphere. The corresponding equations for the maximum escape flux and associated escape parameter at the atmospheric level r_1 where the escape takes place are

$$\mathbf{z}_m = \frac{2}{s+1} \left[\frac{(X_1/2)^{(s+1)/2} + 1}{X_0 - X_1} \right]^2, \quad (12)$$

where X_0 and X_1 are the escape parameters GMm/kT_0r at $r=r_0$ and $r=r_1$. One gets for X_1

$$X_1 = \left\{ \frac{\mathbf{b}}{\mathbf{z}_m} \left[X_0 - \left(\frac{2}{(1+s)\mathbf{z}_m} \right)^{1/2} \right]^{-1} \right\}^{1/2}. \quad (13)$$

The simultaneous solutions of these equations for ζ_m and X_1 must be accomplished by numerical methods with specified values of β and X_0 .

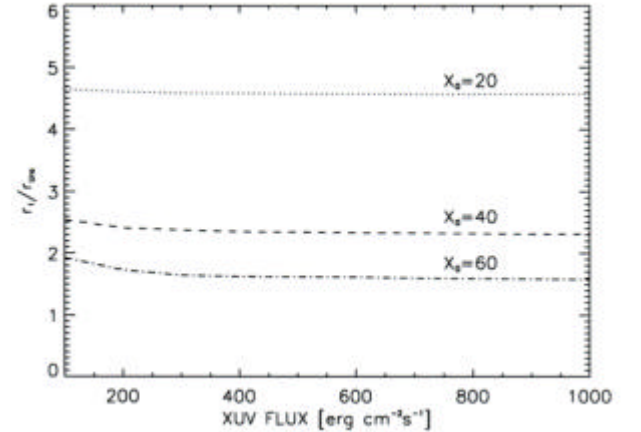


Fig. 1. r_1 in units of Uranus radii r_{Ura} as function of solar XUV energy flux and parameters X_0 between 20 and 60.

Fig. 1 shows values for the radius r_1 in units of r_{Ura} . One can see that the expansion distance r_1 is closer to the planetary radius if X_0 is larger which implicates that r_1 is closer to planetary surface or the defined planetary radius in the case of giant gaseous planets.

4. EVOLUTION OF THE XUV FLUX WITH TIME

The time-dependence of the I_{XUV} flux is very critical for the evolution of thermal escape during the history of a planetary system. Estimates of the solar high-energy flux evolution are indirectly possible by

comparison with solar proxies. Multiwavelength observations have been collected for a sample of solar proxies inside the *Sun in Time* program containing stars, which represent most of the Sun's main sequence lifetime from 130 Myr to 8.5 Gyr [9]. The resulting relative XUV fluxes yield a power-law relationship between 1 Å and 1000 Å of $I_0(t)/I_0 = 6.13 \times [t(\text{Gyr})]^{-1.19}$ and for Lyman- α of $I_{L\alpha}(t)/I_{L\alpha} = 3.17 \times [t(\text{Gyr})]^{-0.75}$. In these expressions, which are valid for ages between 0.1 and 8 Gyr, I_0 and $I_{L\alpha}$ are the present integrated fluxes at 1 au and $I_0(t)$ and $I_{L\alpha}(t)$ are the integrated fluxes as function of time. For our study, we will consider $I_{XUV}(t) = I_0(t) + I_{L\alpha}(t)$. The relationships above are in good agreement with previous studies and indicate from Fig. 2 fluxes of ≈ 6 times I_0 and ≈ 3 times $I_{L\alpha}$ about 3.5 Gyr ago, and ≈ 100 times I_0 and ≈ 20 times $I_{L\alpha}$ about 100 Myr after the Sun's arrival on the main sequence.

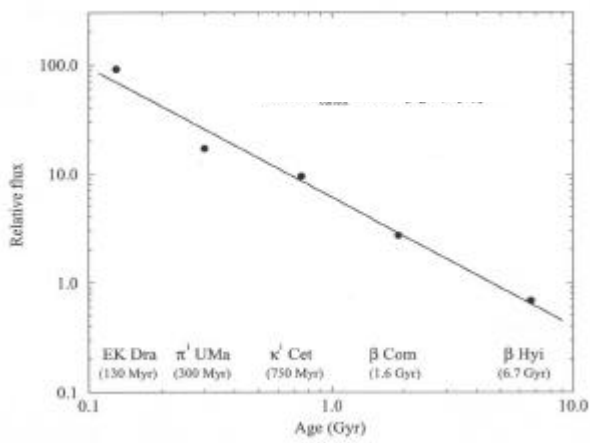


Fig. 2. Evolution of the XUV flux obtained from solar proxies inside the “Sun in Time” program for G-type Sun-like stars.

5. EXOSPHERE TEMPERATURE ESTIMATION

For the estimation of $T_{XUV\infty}$ of migrating Neptune-class exoplanets we use the scaling law of Eq. 5 and the power law of the XUV flux evolution obtained from the study of solar proxies. The dashed lines in Fig. 3 show $T_{XUV\infty}$ for a migrating Uranus-mass exoplanet as a function of distance at present (4.5 Gyr), 1 Gyr, 0.2 Gyr and 0.1 Gyr after the stars arrival on the main sequence. The dotted lines in Fig. 3 show T_∞ by assuming that additional heating sources to be a constant term and the scaled XUV contribution. The dashed-dotted-dotted-dotted lines show T_{eff} , which is much lower at close orbital distances. One can see that the exosphere of such planets will reach blow off conditions ($X \leq 1.5$) even at present low XUV flux values if one considers only the XUV heat contribution

to the exospheric temperature alone. Neptune-class exoplanets with lower masses will reach exospheric blow off conditions at temperatures below 10000 K. It should be noted that the Jeans escape flux and the scaling law are not valid after the exospheric temperature reached values much larger than about 10000 K, because the upper atmosphere expands due to the high temperature and loss rates so that the hydrodynamic treatment must be considered.

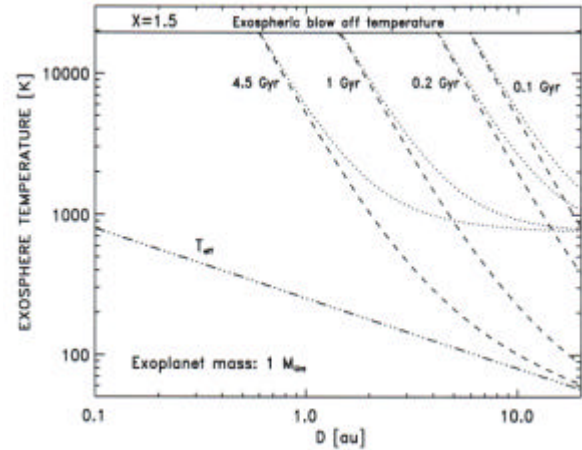


Fig. 3. $T_{XUV\infty}$, T_∞ , and T_{eff} for various XUV flux values as function of distance for a migrating Uranus-mass exoplanet.

The XUV depositing layer may expand up to about 5 planetary radii as shown in Fig. 1. This process is driven by the XUV flux alone. If the planet migrates closer to the host star the XUV flux gets larger, yielding a larger escape flux.

6. ENERGY LIMITED ESCAPE RATES

Because our study suggests that the Jean's approach is not valid for close-in hydrogen rich exoplanets the atmospheric mass loss rates can no longer be estimated from the Jeans equation and hydrodynamic escape must be considered. Thus, the maximal energy-limited loss rate is [8]:

$$L_{\text{Hydro}} = \frac{4\pi r_1^3 I_{XUV}}{GMm}, \quad (14)$$

where I_{XUV} is the effective XUV heat flux averaged over the planetary sphere and r_1 is the radius where the bulk of the XUV flux is absorbed. The distance r_0 is below r_1 but above the planetary surface. The upper loss rate is reached if $r_0 \approx r_1$ which is the case at high XUV fluxes. By using Eq. 14 our calculation yield an energy-limited mass loss rate for HD 209458b in the order of $\approx 10^{10} - 10^{11} \text{ g s}^{-1}$, which is in agreement with the inferred observational based estimation of about 10^{10} g s^{-1} [5]. In contrast, the value resulting from Jeans

escape at T_{eff} is $< 1 \text{ g s}^{-1}$. Fig. 4 shows the atmospheric pressure loss for Neptune-class exoplanets caused by hydrodynamic escape with $1 M_{\text{Ura}}$ (solid lines), $0.5 M_{\text{Ura}}$ (dotted lines) and $3 M_{\text{Earth}}$ (dashed lines) after 1, Gyr. The mass loss in Fig. 5 is expressed as a pressure variation and is given for 3 planetary masses with an estimated expansion radius r_1 of about 5 planetary radii:

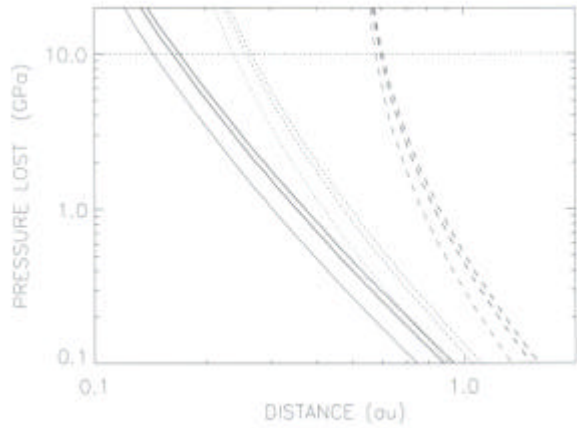


Fig. 4. Evolution of hydrogen atmospheres under energy-limited escape flux conditions for Neptune-class exoplanets as a function of distance and a corresponding XUV deposition layer of about 5 planetary radii.

$1 M_{\text{Ura}}$ (solid lines), $0.5 M_{\text{Ura}}$ (dotted lines) and $3 M_{\text{Earth}}$ (dashed lines), by assuming a density of 1.2 g cm^{-3} . For each planet the pressure potentially lost is given for ages of 1 Gyr (thinnest line), 5 Gyr and 10 Gyr (thicker lines). After 1 Gyr, these planets may lose an atmosphere comparable to the present gaseous hydrogen component of Uranus (10 GPa, dotted line) at 0.15, 0.25 and 0.55 au. One should note that the results in Fig. 4 correspond to an estimated r_1 of about 5 planetary radii. The atmospheric loss would be smaller if the expansion distance is < 5 planetary radii.

7. ION PICK UP BY THE STELLAR WIND

For stellar wind ion pick up one must know the stellar wind density and velocity during the history of the planetary system. The high X-ray activity and the fast rotation of young Sun-like stars indicate a much higher stellar wind in the past. Coronal winds of Sun-like stars were recently indirectly detected [10]. Hubble Space Telescope high spectral resolution observations of H Lyman- α of several nearby main-sequence stars have revealed neutral hydrogen associated with the interaction between their fully ionized coronal winds with the partially ionized local interstellar medium. Models of the associated absorption features, which are formed in the astrospheres, provided the first empirical

estimated coronal mass loss rates from G-K main sequence stars. By using the amount of absorption in the HI area surrounding solar proxies as a diagnostic for their stellar mass loss rates a correlation between the mass loss and X-ray surface flux allows a power law relation, which indicates a solar wind up to 1000 times more massive in the past [10] and shown for an orbital distance of 0.3 au in Fig. 5.

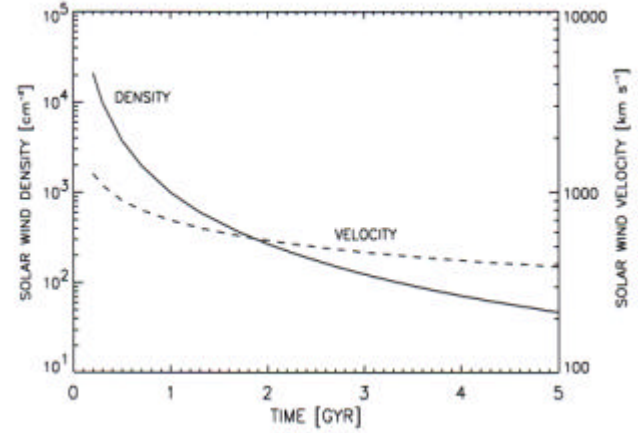


Fig. 5. Change of stellar wind velocity [11] and density [10] over time at an orbital distance of about 0.3 au.

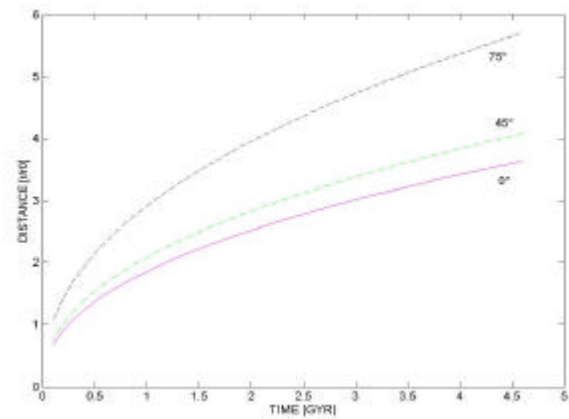


Fig. 6. Compression of Neptune's magnetopause distance without an atmosphere in Neptune radii as function of time and solar zenith angle at an orbital distance of 0.3 au.

Fig. 6 shows the compression of Neptune's magnetopause distance without an atmosphere in planetary radii and as function of time and zenith angle at an orbital distance of 0.3 au. One can see that such a planet would not have been protected by its magnetic field if the atmosphere is expanded due to energy limited escape conditions. The magnetic field strength of 13000 nT corresponds to Neptune's present magnetic field strength. One can see that the magnetic barrier is compressed by the stellar wind below 5 planetary radii, so that a Venus-like stellar wind atmosphere interaction should occur. The total loss of pick up ions

is calculated by means of a test particle model which is based on the proton flow in the magnetosheath according to the *Spreiter-Stahara* model [4, 12]. The production rates of planetary hydrogen ions due to photo-ionization, electron impact and charge exchange are determined by using Neptune's density profile and the stellar wind and XUV conditions shown in Fig. 2 and Fig. 5. The escape fluxes shown in Fig. 7 are calculated by following the trajectories of the newly born hydrogen ions.

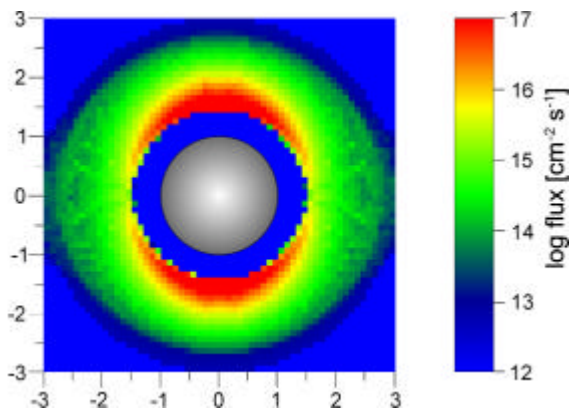


Fig. 7: Hydrogen ion pick up fluxes illustrated through a sphere centred at the planet for a migrated Neptune-class exoplanet at about 0.3 au exposed to a stellar wind over the first Gyr after the star arrived at the main sequence.

One can see from Fig. 7 that very high non-thermal ion-pick up escape fluxes and hydrogen loss rates can be reached, due to an expanded atmosphere up to about $5 \times 10^{36} \text{ s}^{-1}$. It should be noted that these results are preliminary and depend on the XUV driven expansion of the thermosphere. A lower expansion would give a lower pick up ion loss rate. Future studies will include a detailed connection between the hydrodynamic treatment and non-thermal pick up ion loss simulations.

8. CONCLUSION

Our preliminary studies imply that Neptune-class exoplanets, because of the higher stellar I_{XUV} irradiance and stellar wind in the past and/or a close distance to their host star, can lose their entire hydrogen atmospheres due to non-thermal and thermal escape processes. Due to an XUV driven expanded atmosphere a Venus-like solar wind interaction may occur during the whole lifetime, because their magnetospheres are compressed due to the higher stellar wind close to the star. Thus, these planets could evolve into a new class of “terrestrial planets”, which could be detected with the new generation of space observatories like COROT and Eddington.

ACKNOWLEDGEMENTS

H. Lammer thanks J. Linsky from the University of Colorado, Boulder, USA for interesting discussions regarding stellar winds. W. W. Weiss thanks the Austrian Ministry for Science, Education and Culture (bm:bwk) for supporting the COROT project. E. F. Guinan and I. Ribas acknowledge support from NASA/FUSE grants NAG5-10387 and NAG5-12125.

REFERENCES

1. Konacki, M., et al. A new transiting extrasolar giant planet. *NATURE*, Vol. 421, 137-143, 2003.
2. Sasselov, D. D. The new transiting OGLE-TR-56b: Orbit and atmosphere. *AP. J. LETT.* submitted, 2003.
3. Bauer, S. J. Solar cycle variation of planetary exospheric temperatures. *NATURE*, Vol. 232, 101-102, 1971.
4. Lichtenegger, H. I. M., et al. Energetic neutral atoms at Mars III. Flux and energy distributions of planetary energetic H atoms, *J. GEOPHYS. RES.*, Vol. 107 (A10), 1279, doi:10.1029/2001JA000322., 2002.
5. Vidal-Madjar, A., et al. An extended upper atmosphere around the extrasolar planet HD209458b. *NATURE*, Vol. 422, 143-146, 2003.
6. Bauer, S. J. and Hantsch, M. H. Solar cycle variation of the upper atmosphere temperature of Mars. *GEOPHYS. RES. LETT.*, Vol. 16, 373-376, 1989.
7. Öpik, E. J. Selective escape of gases. *GEOPHYS. J. ROY. ASTRON. SOC.*, Vol 7, 490, 1963.
8. Watson, A. J. et al. The dynamics of a rapidly escaping atmosphere: applications to the evolution of Earth and Venus. *ICARUS*, Vol. 48, 150-166, 1981.
9. Guinan, E. F. Ribas I. in *The evolving Sun and its Influence on Planetary Environments*, ASP, Vol. 269, 85-107, 2002.
10. Wood, B. E. et al., Measured mass loss rates of solar-like stars as a function of age and activity, *AP. J.*, Vol. 574 (1), 412-425, 2002.
11. Newkirk Jr., G. Solar variability on time scales of 105 years to 109.6 years. *GEOCHI. COSMOCHI. ACTA SUPPL.*, Vol. 13, 293-301, 1980.
12. Spreiter, J. R., and S. S. Stahara 1980. Solar wind flow past Venus: Theory and comparisons. *J. GEOPHYS. RES.*, Vol. 98, 17,251-17,262, 1980.